Histol Histopathol (2022) 37: 227-241

http://www.hh.um.es

Histology and Histopathology
From Cell Biology to Tissue Engineering

ORIGINAL ARTICLE **Open Access**

CircAKT3 promotes cell proliferation, survival and glutamine metabolism of gastric cancer by activating SLC1A5 expression via targeting miR-515-5p

Fei Li[1], Lixiao Zhang[2] and Qi Sun[3]

[1]Department of Clinical Laboratory, Taizhou Central Hospital (Taizhou University Hospital), Taizhou, [2]Department of Gastrointestinal Surgery, Hebei General Hospital, Shijiazhuang and [3]Third Ward, Cancer Center, THE PLA NAVY ANQING, Anqing, China

Summary. Background. Gastric cancer (GC) is a common disorder in the population. Numerous studies have reported that the pathogenesis of GC is implicated in the dysregulation of circular RNAs (circRNAs). The aim of this study was to investigate the role and functional mechanism of circ_0000199 (circAKT3) in GC.

Methods. The expression of circAKT3, miR-515-5p and solute carrier family 1 member 5 (SLC1A5) mRNA was measured by quantitative real-time PCR (qPCR). Cell proliferation was assessed by cell counting kit-8 (CCK-8) assay, colony formation assay and 5-ethynyl-2'-deoxyuridine (EdU) assay. Cell apoptosis was determined by flow cytometry assay and caspase 3/7 activity. The protein levels of glutaminase (GLS), proliferating cell nuclear antigen (PCNA) and cleaved-caspase3 were detected by western blot. The binding relationship between miR-515-5p and circAKT3 or SLC1A5 was verified by dual-luciferase reporter assay or RIP assay. The role of circAKT3 in vivo was investigated by establishing animal models. The abundance of Ki-67 and PCNA was detected by IHC assay.

Results. The expression of circAKT3 in GC tissues and cells was enhanced. The knockdown of circAKT3 inhibited GC cell proliferation, survival and glutamine metabolism, as well as tumor growth in animal models. MiR-515-5p was a target of circAKT3, and miR-515-5p suppressed the expression of SLC1A5 by binding to SLC1A5 3'UTR. CircAKT3 relieved the inhibition of miR-515-5p on SLC1A5 expression by targeting miR-515-5p. The effects of circAKT3 knockdown were reversed by miR-515-5p depletion, and the effects of miR-515-5p restoration were abolished by SLC1A5 overexpression.

Conclusion. CircAKT3 promotes the malignant development of GC by activating SLC1A5 expression via targeting miR-515-5p.

Key words: circAKT3, Gastric cancer, miR-515-5p, SLC1A5

Corresponding Author: Qi Sun, Third Ward, Cancer Center, THE PLA NAVY ANQING, No. 150, Shuangjing Street, Anqing 246003, Anhui, China. e-mail: sunqi_116@163.com

DOI: 10.14670/HH-18-401

Introduction

The burden of gastric cancer (GC) incidence and mortality is increasing worldwide. GC is the fifth most commonly diagnosed cancer and the fourth leading cause of cancer-related deaths in global cancer statistics 2020 (Sung et al., 2021). The unsatisfactory outcome of GC treatment is attributed to late diagnosis and frequent metastasis (Feng et al., 2019). GC is a disease of high molecular and phenotypic heterogeneity, and its development is regulated by numerous oncogenic drivers, such as non-coding RNAs (ncRNAs) (Smyth et al., 2020; Wei et al., 2020). Therefore, in-depth studies of ncRNAs can expand the insights into the understanding of GC pathogenesis and provide new strategies for GC treatment.

The study of circular RNAs (circRNA) has attracted public attention in recent years. CircRNAs represent a class of ncRNAs, with unique circular structures, which confer them irreplaceable biological characteristics, such as high stability (Ruan et al., 2020). Increasing circRNA expression profiles manifest that numerous circRNAs are aberrantly expressed in GC, and altered circRNA expression is closely associated with the clinicopathologic features of GC patients, hinting at the potency of circRNAs as biomarkers for GC diagnosis and prognosis (Tang et al., 2019; Khanipouyani et al., 2021). For example, high circMRPS35 expression was correlated with good prognosis of GC patients, and circMRPS35 overexpression inhibited the growth and metastasis of GC in vitro and in vivo (Jie et al., 2020). On the contrary, high circLMTK2 expression was

associated with poor prognosis, advanced stage and metastasis, and circLMTK2 overexpression induced GC cell migration and invasion (Wang et al., 2019a,b). CircAKT3 (circ_0000199), produced by back-splicing from AKT serine/threonine kinase 3 (AKT3) mRNA, has been confirmed to play wide functions in various cancers (Huang et al., 2019; Luo et al., 2020). It was previously identified to be highly expressed in GC tumor tissues with cisplatin resistance by RNA sequencing (Huang et al., 2019), suggesting that circAKT3 deregulation was associated with GC progression. However, the functional mechanism of circAKT3 in GC is not fully understood.

It is canonical that endogenous circRNAs act as a molecular sponge to inhibit the expression of target microRNAs (miRNAs), thus relieving the inhibition of miRNAs on downstream target genes (Liu et al., 2017). The public bioinformatics tools easily predict the potential target miRNAs of circRNA, as well as target genes of miRNA, such as circinteractome and starbase (Li et al., 2014; Dudekula et al., 2016). MiR-515-5p was predicted as a target of circAKT3, and the involvement of miR-515-5p in GC development has been partly elucidated (Zhang et al., 2019a,b; Wang et al., 2020). We speculated that miR-515-5p was involved in circ_AKT3-mediated regulatory networks. In addition, solute carrier family 1 member 5 (SLC1A5, also known as ASCT2) was analyzed to be a potential target of miR-515-5p. SLC1A5 is essential for glutamine transport and has been widely reported to participate in cancer development, including GC (Ye et al., 2018). However, the interaction between miR-515-5p and SLC1A5 has not been not explored in any cancers.

Here, we verified the expression of circAKT3 in tumor tissues and cell lines of GC. Besides, loss-of-function assays were performed to explore the role of circAKT3 in GC cells and animal models. Moreover, we performed rescue experiments to construct the circAKT3/miR-515-5p/SLC1A5 network. Our study aimed to provide more evidence for circAKT3 to participate in GC development and address a novel regulatory mechanism of circAKT3.

Materials and methods

Clinical tissues

Patients diagnosed with GC at Taizhou Central Hospital were enrolled in this study. Patients never received any treatments prior to the surgical operation. A total of 61 pairs of tumor tissues and matched normal tissues were used in this study, and all patients provided written informed consent. Tissues used in our study were selected according to the following exclusion criteria: (1) patients had received any therapies, and (2) patients had other cancers or systemic diseases. These samples were preserved at -80□ conditions until use. Our study obtained the permission of the Ethics Committee of Taizhou Central Hospital.

Cell lines

Common GC cell lines, including MKN-7 and HGC-27, were purchased from EK-Bioscience (Shanghai, China) and cultured in RPMI1640+10% FBS (GIBCO, Grand Island, NY, USA) or DMEM+10% FBS (GIBCO), respectively. Human gastric mucosal epithelial cells (GES-1; non-cancer control) were also obtained from EK-Bioscience and cultured in DMEM+10% FBS. Human embryonic kidney cells (293T) were purchased from Sigma-Aldrich (St. Louis, MO, USA) and cultured in DMEM+10% FBS.

Cell transfection

CircAKT3 knockdown was mediated by short hairpin RNA (sh-circAKT3) that was synthesized by Genepharma (Shanghai, China), with sh-NC as a negative control. MiR-515-5p restoration or inhibition was mediated by miR-515-5p mimic (miR-515-5p) or miR-515-5p inhibitor (anti-miR-515-5p) that were directly purchased from Ribobio (Guangzhou, China), with miR-NC or anti-miR-NC as the matched negative control. SLC1A5 overexpression was mediated by pcDNA-SLC1A5 overexpression vector (Genepharma), with pcDNA-NC blank vector as the control. Transfection or cotransfection (oligonucleotide: 50 nM; vector: 1 μg) was conducted in cells using the Lipofectamine 3000 reagent (Invitrogen, Carlsbad, CA, USA).

Quantitative real-time PCR (qPCR)

Trizol reagent (Invitrogen) was used to extract total RNA. Then, total RNA (2 μg) was subjected to reverse transcription using the PrimeScript RT reagent kit (Takara, Dalian, China) or using the TaqMan MiRNA Reverse Transcription kit (Applied Biosystems, Foster City, CA, USA) as appropriate. Subsequently, cDNA was amplified and quantified using the SYBR Green Master PCR mix (Takara). Relative expression was normalized by GAPDH or U6, and the $2^{-\Delta\Delta Ct}$ method was applied for calculation. The sequences of primers were shown as follows:

circAKT3, F: 5'-TATATGATAAAAAGCTG-3' and R: 5'-TCTTTCCGGAATGTAGATA-3'; AKT3, F: 5'-ACCCATGGAACTGTTGGCTT-3' and R: 5'-TTCGAGTTAACGTGCCTGCT-3'; GAPDH, F: 5'-GGAGTCCACTGGCGTCTTCA-3' and R: 5'-GGTTCACACCCATGACGAAC-3'; miR-515-5p, F: 5'-GCGTTCTCCAAAAGAAAGCAC-3' and R: 5'-AGTGCAGGGTCCGAGGTATT-3'; U6, F: 5'-CTCGCTTCGGCAGCACATATACT-3' and R: 5'-ACGCTTCACGAATTTGCGTGTC-3'; SLC1A5, F: 5'-ACTCGACAGGATATTGAGGGGA-3' and R: 5'-TGCTGACACCAGGTTGGAAG-3'.

RNase R treatment and Actinomycin D (ActD) treatment

Total RNA isolated from MKN-7 and HGC-27 cells

was incubated with RNase R (3 U/μg; Epicentre Technologies, Madison, WI, USA) at 37□ for 0.5 h. The treated RNA was used for qPCR analysis.

MKN-7 and HGC-27 cells were exposed to Actinomycin D (2 μg/mL; Sigma-Aldrich) for different times (0, 8, 12 and 24 h). The treated cells were collected for RNA isolation, followed by qPCR analysis.

Cell counting kit-8 (CCK-8) assay

Cell viability at the indicated time points after transfection was checked using CCK-8 reagent (Sigma-Aldrich). Cells after transfection were seeded into 96-well plates (2,000 cells/well) and treated with 10 μL CCK-8 reagent at 0, 1, 2 and 3 days post-incubation. The absorbance at 450 nm was measured by a microplate reader (BioTek, Biotek Winooski, Vermont, USA).

Colony formation assay

Cells after transfection were seeded into 6-well plates (200 cells/well) and then cultured at 37□ conditions containing 5% CO_2 for 2 weeks. Cell colonies were stained with 0.1% crystal violet (Beyotime, Shanghai, China) and observed under a microscope (Leica, Wetzlar, Germany).

5-ethynyl-2'-deoxyuridine (EdU) assay

EdU assay kit (RiboBio, Guangzhou, China) was used to assess cell proliferation. 50 μM EdU labeling medium was added to incubate cells in 96-well plates (2,000 cells/well) for 2 h. The cultured cells were fixed with 4% paraformaldehyde, and 1 × Apollo reaction cocktail was added to react with EdU for 30 min. DAPI was then added to stain cell nucleus. The number of EdU-positive cells in five random fields in each well was counted under a fluorescent microscope (Leica).

Flow cytometry assay

Annexin V-FITC Apoptosis Staining / Detection Kit (Abcam, Cambridge, MA, USA) was applied to detect cell apoptosis. Cells after transfection were cultured for 48 h and then collected after trypsin digestion. Cells were resuspended in 500 μL of 1× Annexin V Binding Buffer and then stained with 5 μL Annexin V-FITC and 5 μL propidium iodide (PI). After that, the apoptotic cells were analyzed by a flow cytometer (Beckman, Miami, FL, USA).

Caspase3/7 activity detection

Caspase activity assay for apoptosis detection was determined using Caspase-Glo® 3/7 Assay System (Promega, Madison, WI, USA) according to the directions. In brief, cells in 96-well plates were treated with equal volumes of Caspase-Glo® 3/7 reagent for 2 h. The luminescence was recorded using a GloMax System (Promega).

Glutamine uptake assay

The content of glutamine in culture medium was measured using a Glutamate Assay Kit (Abcam) according to the protocol. Glutamine uptake of the experimental cells was calculated according to the content of glutamine in culture medium.

Western blot

Glutaminase (GLS) is a marker yielding glutamate from glutamine. Proliferating cell nuclear antigen (PCNA) is a marker of active cell proliferation. Cleaved-caspase3 is a marker of cell apoptosis. The primary antibodies targeting GLS (ab260047), PCNA (ab92552), pro-caspase3 (ab32150), cleaved-caspase3 (ab32042), SLC1A5 (ab237704) and GAPDH (ab9485) were purchased from Abcam, using Goat Anti-Rabbit IgG (ab205718) as the secondary antibody. The standard procedures of western blot were performed. The signals on the membranes were presented using the ECL reagent (Beyotime).

Bioinformatics analysis and dual-luciferase reporter assay

Bioinformatics tool, circinteractome (https://circinteractome.nia.nih.gov/) and starbase (http://starbase.sysu.edu.cn/) were used for target prediction. The wild-type (wt) and the mutant-type (mut) sequence of circAKT3 (containing wt miR-515-5p binding site or mut miR-515-5p binding site) were amplified and inserted into pmirGLO plasmid to construct circAKT3 wt and circAKT3 mut reporter plasmids (Genepharma). Similarly, SLC1A5 3'UTR wt and SLC1A5 3'UTR mut reporter plasmids were also constructed. 293T cells were transfected with the WT or MUT reporter plasmid of circAKT3 or SLC1A5 3'UTR (1 μg) and miR-515-5p or miR-NC (50 nM) and cultured for 48 h after transfection. Luciferase activity was then ascertained using the Dual-Luciferase Reporter Assay System (Promega, Madison, WI, USA).

RNA immunoprecipitation (RIP) assay

Utilizing the Magna RIP Kit (Millipore, Billerica, MA, USA), 293T cells were lysed and cell lysates were exposed to Ago2 antibody-conjugated or IgG antibody-conjugated magnetic beads. RNA complex on beads was eluted and isolated using Trizol reagent, followed by qPCR assay to detect the enrichment of circAKT3 and miR-515-5p.

Animal models

The procedures of animal study were approved by the Animal Care and Use Committee of Taizhou Central

Hospital. Balb/c mice aged 6-week-old (Balb/c; female) were purchased from Vital River Laboratory Animal Technology Co., Ltd (Beijing, China). Huh-7 cells were infected with lentivirus-packaged sh-circAKT3 for stable circAKT3 downregulation, with sh-NC as a negative control. To induce a xenograft model, the infected Huh-7 cells (2×10^6 cells per mouse) were subcutaneously inoculated into nude mice (n=5 per group). During tumor development, tumor volume (length×width^2×0.5) was measured once a week. Tumor was allowed to grow for 4 weeks. After that, all mice were euthanized. Tumor tissues were excised, frozen and preserved at -80°C conditions.

Immunohistochemistry (IHC) assay

Paraffin-embedded tissue sections (4-μm-thick) were prepared. Tissues sections were deparaffinized in xylene and rehydrated in graded ethanol. After antigenic retrieval, tissue sections were incubated with the primary antibodies, including anti-ki-67 (ab16667; Abcam) and anti-PCNA (ab92552; Abcam), and subsequently incubated with the secondary antibody (ab205718). After that, tissue sections were stained with DAB (3, 3'-diaminobenzidine; Beyotime) and observed under a microscope (Leica).

Statistical analysis

All experiments were independently repeated three times. Data were represented as mean±SD. Student's t-tests were used to compare the difference between two groups. Analysis of variance (ANOVA) was used for difference comparison among various groups. Linear correlation between two sets was analyzed by Pearson's correlation analysis. All data were analyzed by GraphPad Prism 7.0 (GraphPad Software, Inc.). P value <0.05 was considered statistically significant.

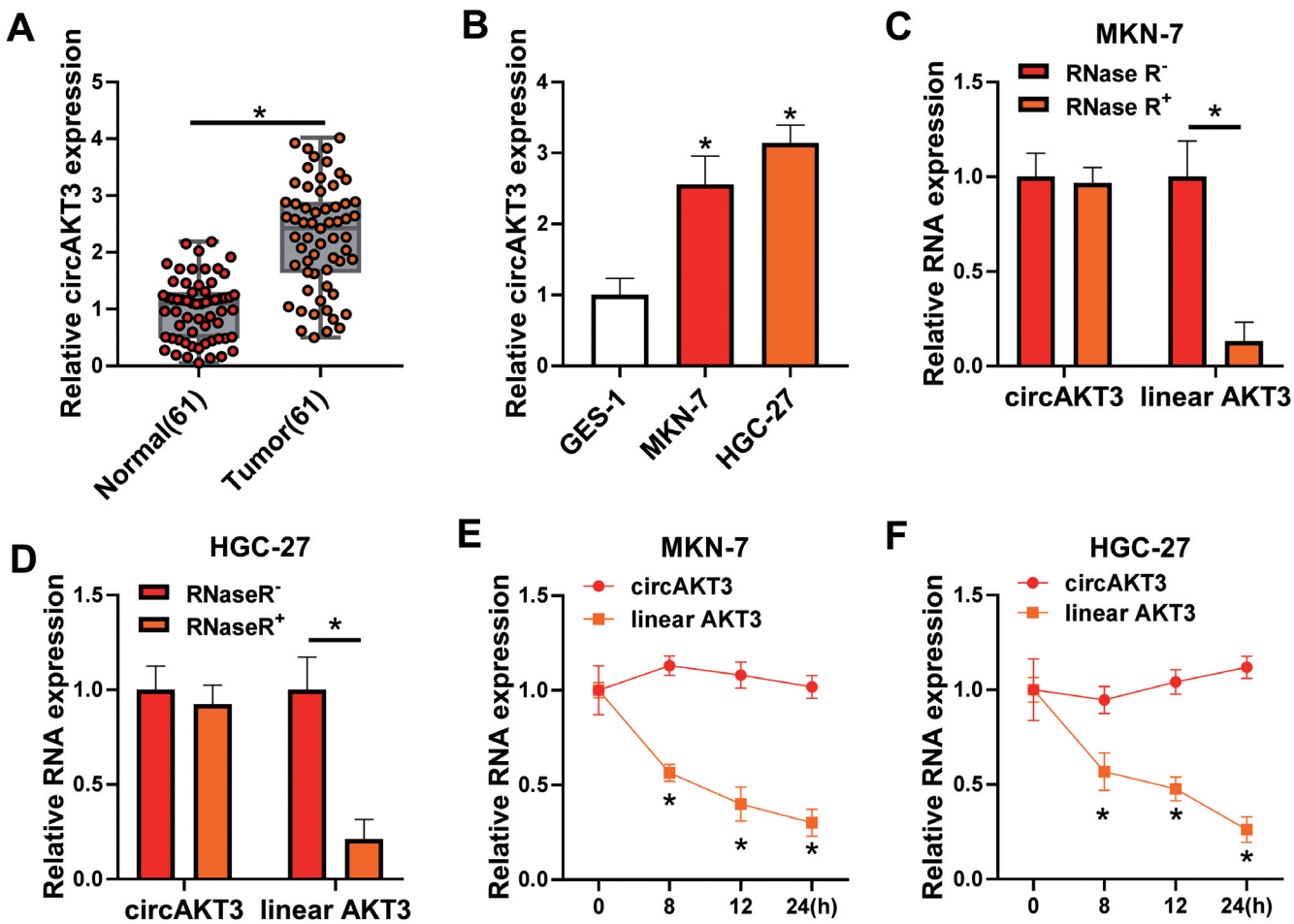

Fig. 1. CircAKT1 was overexpressed in tumor tissues and cells of GC. **A.** The expression of circAKT1 in tumor tissues and normal tissues. **B.** The expression of circAKT1 in GES-1, MKN-7 and HGC-27 cells. **C, D.** The stability of circAKT1 was checked by RNase R. **E, F.** The stability of circAKT1 was checked by Actinomycin D. *P<0.05.

Results

CircAKT3 was upregulated in GC tumor tissues and cells

The data from qPCR clearly showed that the expression of circAKT3 was notably increased in clinical tumor tissues (n=61) compared to normal tissues (n=61) (Fig. 1A; P<0.05). Besides, its expression was also notably enhanced in MKN-7 and HGC-27 cells compared with that in GES-1 cells (Fig. 1B; P<0.05). Fig. 2 provided the information that circAKT3 was derived from the exon8, exon9, exon10 and exon11 regions of AKT3 gene by back-splicing mechanism, with 555 nucleotides in length. RNase R and ActD were used to further identify circAKT3. The data showed that circAKT3 was hardly digested by RNase R and ActD, while linear AKT3 was substantially degraded by RNase R and ActD (Fig. 1C-1F; P<0.05). These data highlighted that circAKT3 was overexpressed in GC tissues and cells.

The knockdown of circAKT3 suppressed proliferation, survival and glutamine metabolism in GC cells

The expression of circAKT3 was pronouncedly declined in MKN-7 and HGC-27 cells by transfecting sh-circAKT3, with si-NC as a control (Fig. 3A; P<0.05). In terms of function, we found that circAKT3 knockdown significantly inhibited cell viability at 3 days post-transfection by CCK-8 assay (Fig. 3B; P<0.05), reduced colony formation ability by colony formation assay (Fig. 3C; P<0.05) and lessened the number of EdU-positive cells by EdU assay (Fig. 3D; P<0.05), suggesting that circAKT3 knockdown inhibited the proliferative capacity of MKN-7 and HGC-27 cells. In addition, flow cytometry assay displayed that circAKT3 knockdown promoted the apoptosis rate of MKN-7 and HGC-27 cells (Fig. 4A; P<0.05), which was verified by the increased caspase3/7 activity in MKN-7 and HGC-27 cells after circAKT3 knockdown (Fig. 4B; P<0.05), suggesting that circAKT3 knockdown inhibited GC cell survival. Moreover, our data discovered that glutamine uptake of MKN-7 and HGC-27 cells was strikingly suppressed by circAKT3 knockdown (Fig. 4C; P<0.05). Several markers related to glutamine, proliferation and apoptosis were quantified by western blot. The data showed that the protein levels of GLS and PCNA were decreased, while the level of cleaved-caspase3 was increased in MKN-7 and HGC-27 cells transfected with

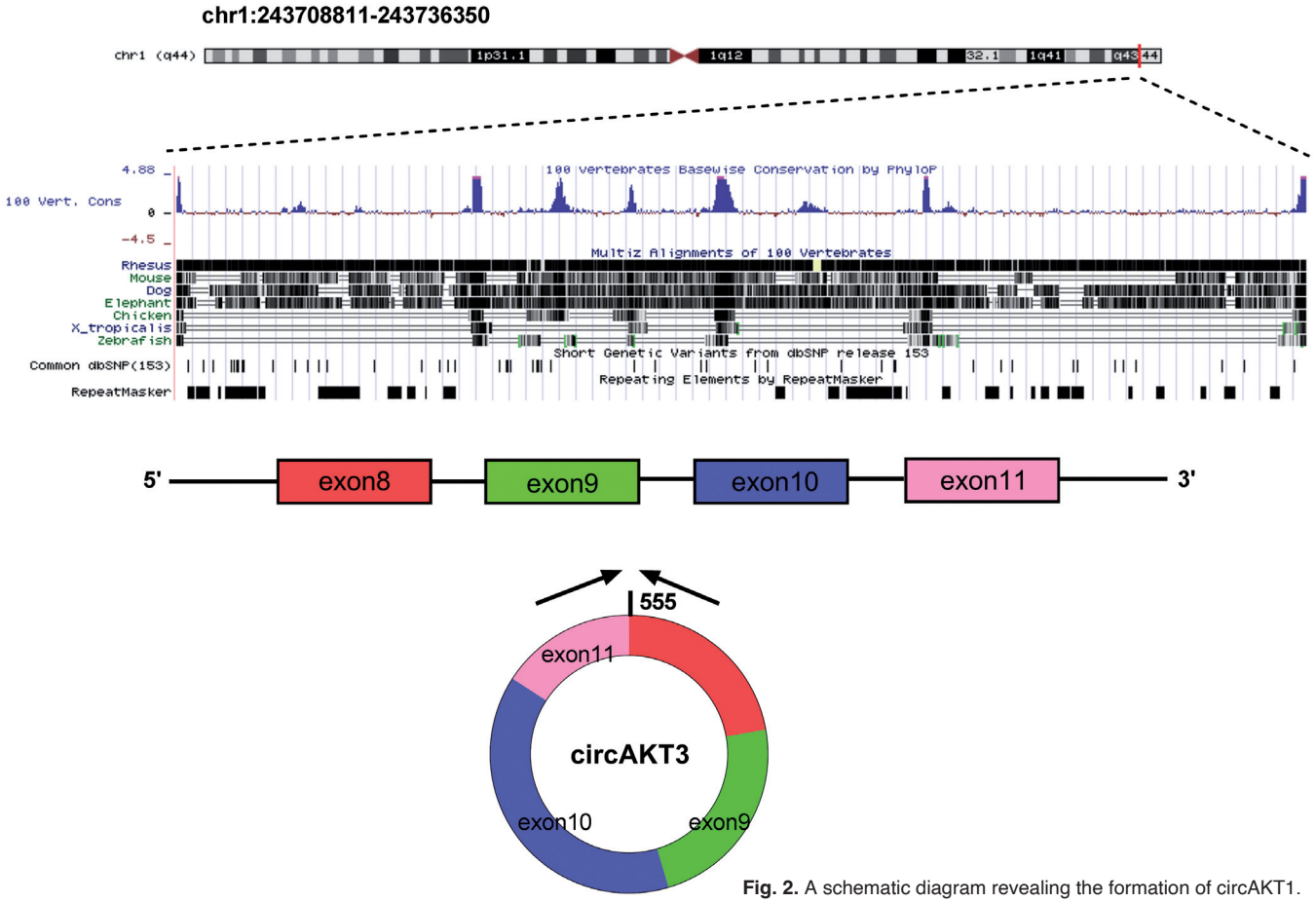

Fig. 2. A schematic diagram revealing the formation of circAKT1.

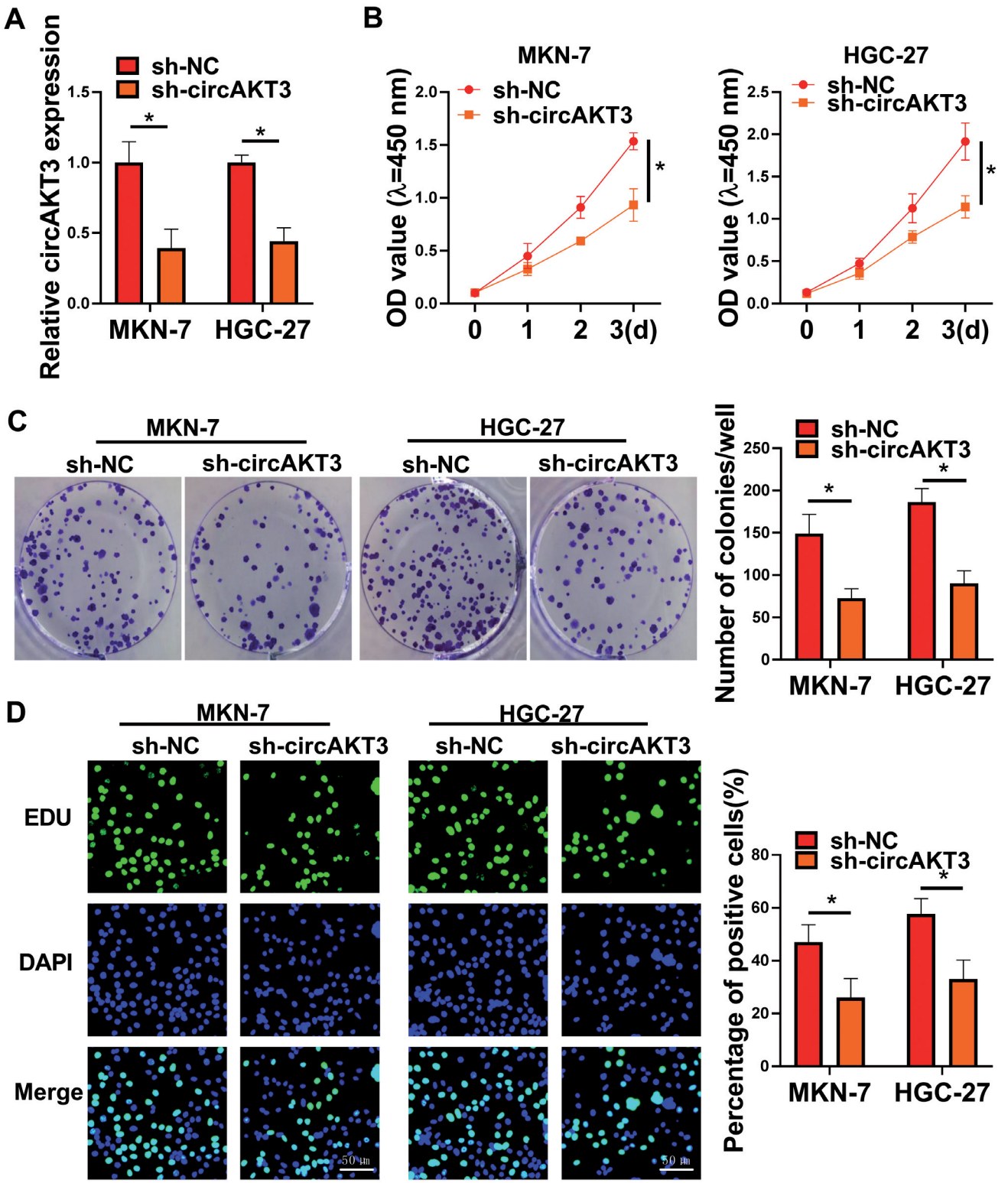

Fig. 3. CircAKT1 knockdown inhibited GC cell proliferation. **A.** The expression of circAKT1 in MKN-7 and HGC-27 cells transfected with sh-circAKT1 or sh-NC. **B.** cell proliferation assessed by CCK-8 assay. **C.** Cell proliferation assessed by colony formation assay. **D.** Cell proliferation assessed by EdU assay. *P<0.05.

sh-circAKT3 (Fig. 4D; P<0.05). Overall, the data suggested that the knockdown of circAKT3 suppressed proliferation, survival and glutamine metabolism in GC cells.

MiR-515-5p, a target of circAKT3, was downregulated in GC tumor tissues and cells

We explored the canonical "sponge" effects of circRNA to determine the functional mechanism of circAKT3 in GC. The data from circinteractome presented that miR-515-5p was one of the targets of circAKT3, with a special binding site on circAKT3 sequence (Fig. 5A). Dual-luciferase reporter assay verified the binding between circAKT3 and miR-515-5p because miR-515-5p mimic combined with circAKT3 wt significantly reduced luciferase activity in 293T cells (Fig. 5B; P<0.05). Besides, circAKT3 and miR-515-5p were enriched in the Ago2-coupled RNA complex in RIP assay (Fig. 5C; P<0.05). The expression of miR-515-5p was notably decreased in tumor tissues (n=61) compared to normal tissues (n=61), and its expression was also notably decreased in MKN-7 and HGC-27 cells compared to GES-1 cells (Fig. 5D,E; P<0.05). In GC tumor tissues, miR-515-5p expression presented a negative correlation with circAKT3 expression (Fig. 5F; P<0.001).

CircAKT3 knockdown weakened its sponge effects on miR-515-5p

We next explored the binding between circAKT3 and miR-515-5p in function. The expression of miR-515-5p was notably decreased in MKN-7 and HGC-27 cells transfected with anti-miR-515-5p (Fig. 6A; P<0.05). The expression of miR-515-5p in MKN-7 and HGC-27 cells was promoted by sh-circAKT3 transfection but repressed by sh-circAKT3+anti-miR-

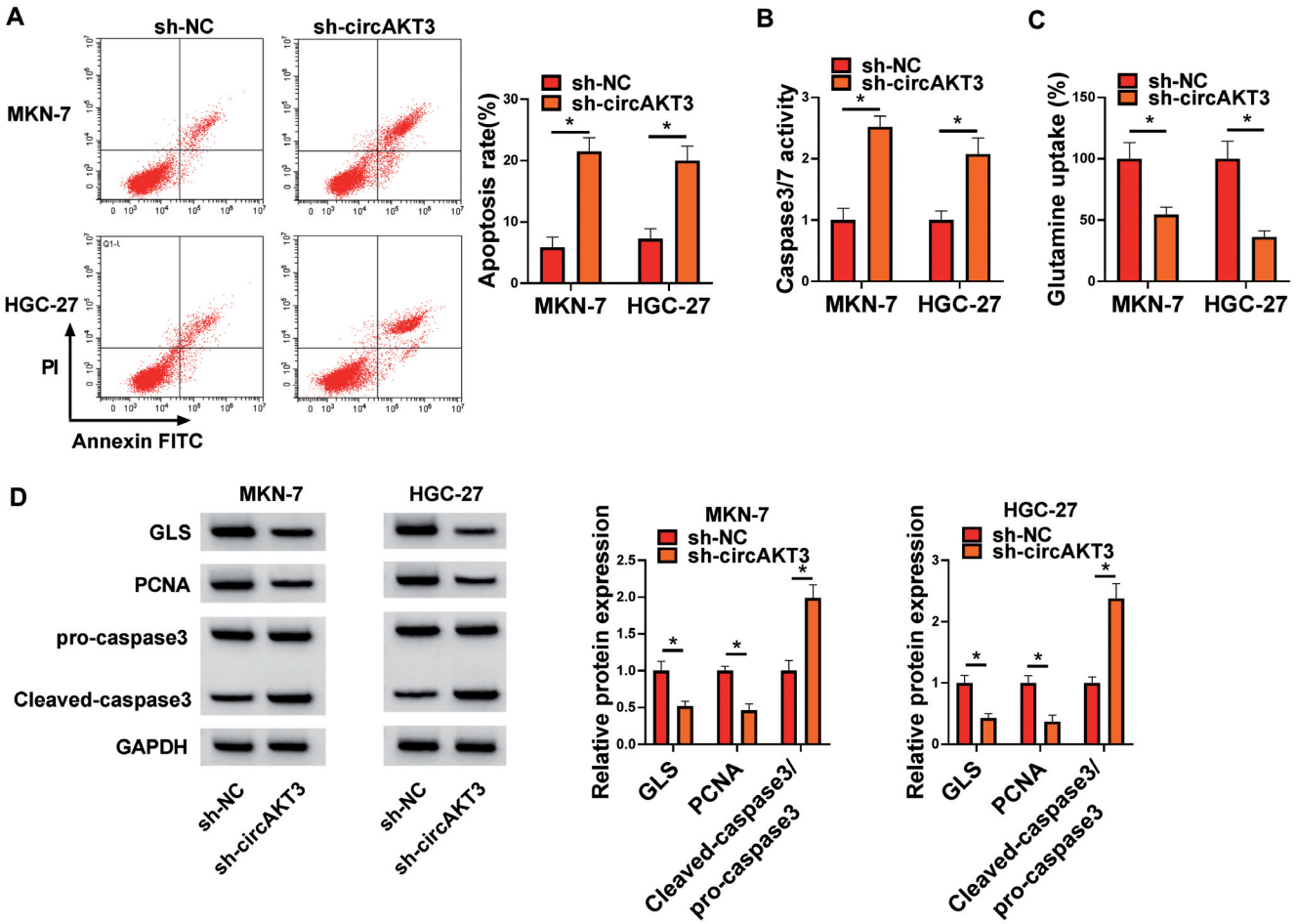

Fig. 4. CircAKT1 knockdown induced GC cell apoptosis and inhibited glutamine uptake. **A.** Cell apoptosis assessed by flow cytometry assay. **B.** Cell apoptosis assessed by caspase3/7 activity assay. **C.** Glutamine uptake detected by a commercial kit. **D.** The protein levels of GLS, PCNA and cleaved-caspase3. *P<0.05.

515-5p transfection (Fig. 6B; P<0.05). In function, the value of OD, the number of colonies and the number of EdU-positive cells decreased by circAKT3 knockdown were largely recovered by the deficiency of miR-515-5p (Fig. 6C,E; P<0.05), suggesting that circAKT3 knockdown inhibited MKN-7 and HGC-27 cell proliferation by enriching miR-515-5p. In addition, circAKT3 knockdown-induced cell apoptosis rate was substantially suppressed by miR-515-5p inhibition, and circAKT3 knockdown-enhanced caspase3/7 activity was also reduced by miR-515-5p inhibition (Fig. 6F,G and Fig. 7; P<0.05). Moreover, glutamine uptake of MKN-7 and HGC-27 cells was suppressed by the knockdown of circAKT3 but largely restored by the inhibition of miR-515-5p (Fig. 6H; P<0.05). The protein levels of GLS and PCNA were notably decreased in MKN-7 and HGC-27 cells by sh-circAKT3 transfection but recovered by sh-circAKT3+anti-miR-515-5p transfection, while the protein level of cleaved-caspase3/pro-caspase3 was notably enhanced in MKN-7 and HGC-27 cells by sh-circAKT3 transfection but repressed by sh-circAKT3+anti-miR-515-5p transfection (Fig. 6I; P<0.05). The data manifested that circAKT3 knockdown weakened its sponge effects on miR-515-5p, thus inhibiting the malignant behaviors of GC cells.

CircAKT3 acted as sponge of miR-515-5p to enrich the expression of SLC1A5

Bioinformatics tool starbase presented that miR-515-5p held the binding site with the 3'UTR of SLC1A5 (Fig. 8A). Dual-luciferase reporter assay displayed that the cotransfection of miR-515-5p and SLC1A5 3'UTR wt significantly reduced luciferase activity in 293T cells (Fig. 8B; P<0.05). The expression of SLC1A5 mRNA and protein was markedly increased in tumor tissues (n=61) compared with that in normal tissues (n=61) (Fig. 8C,D; P<0.05). The expression of SLC1A5 protein was also markedly increased in MKN-7 and HGC-27 cells compared with that in GES-1 cells (Fig. 8E; P<0.05). Additionally, SLC1A5 mRNA expression in GC tumor tissues was negatively correlated with miR-515-5p expression (Fig. 8F; P<0.001). More importantly, we discovered that the expression of SLC1A5 protein was remarkably declined in MKN-7 and HGC-27 cells transfected with sh-circAKT3 but substantially

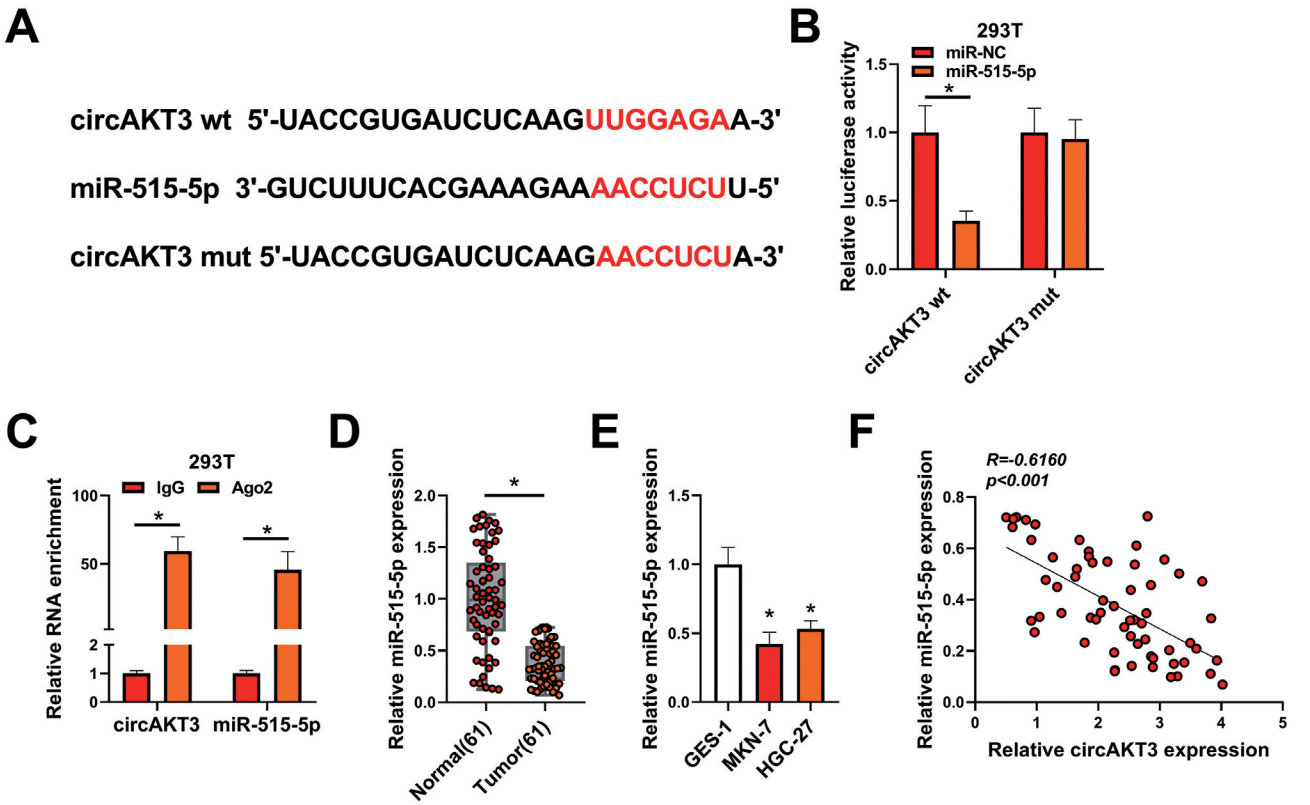

Fig. 5. MiR-515-5p, a target of circAKT3, was downregulated in GC tissues and cells. **A.** The binding site and mutant binding site between circAKT3 and miR-515-5p. **B.** The binding between circAKT3 and miR-515-5p was verified by dual-luciferase reporter assay. **C.** The interaction between circAKT3 and miR-515-5p was verified by RIP assay. **D.** The expression of miR-515-5p in tumor tissues and normal tissues. **E.** The expression of miR-515-5p in GES-1, MKN-7 and HGC-27 cells. **F.** The linear correlation between miR-515-5p and circAKT3. *P<0.05.

recovered in cells transfected with sh-circAKT3+anti-miR-515-5p (Fig. 8G; P<0.05). The data suggested that circAKT3 acted as sponge of miR-515-5p to enrich the expression of SLC1A5.

MiR-515-5p overexpression inhibited GC cell proliferation, survival and glutamine metabolism by depleting SLC1A5

The expression of SLC1A5 protein was notably enhanced in MKN-7 and HGC-27 cells transfected with pcDNA-SLC1A5 compared to pcDNA-NC (Fig. 9A; P<0.05). The expression of miR-515-5p was substantially increased in MKN-7 and HGC-27 cells transfected with miR-515-5p compared to miR-NC (Fig. 9B; P<0.05). The expression of SLC1A5 protein depleted in MKN-7 and HGC-27 cells transfected with miR-515-5p alone was largely recovered in cells transfected with miR-515-5p+pcDNA-SLC1A5 (Fig. 9C; P<0.05). Functional assays were performed in these

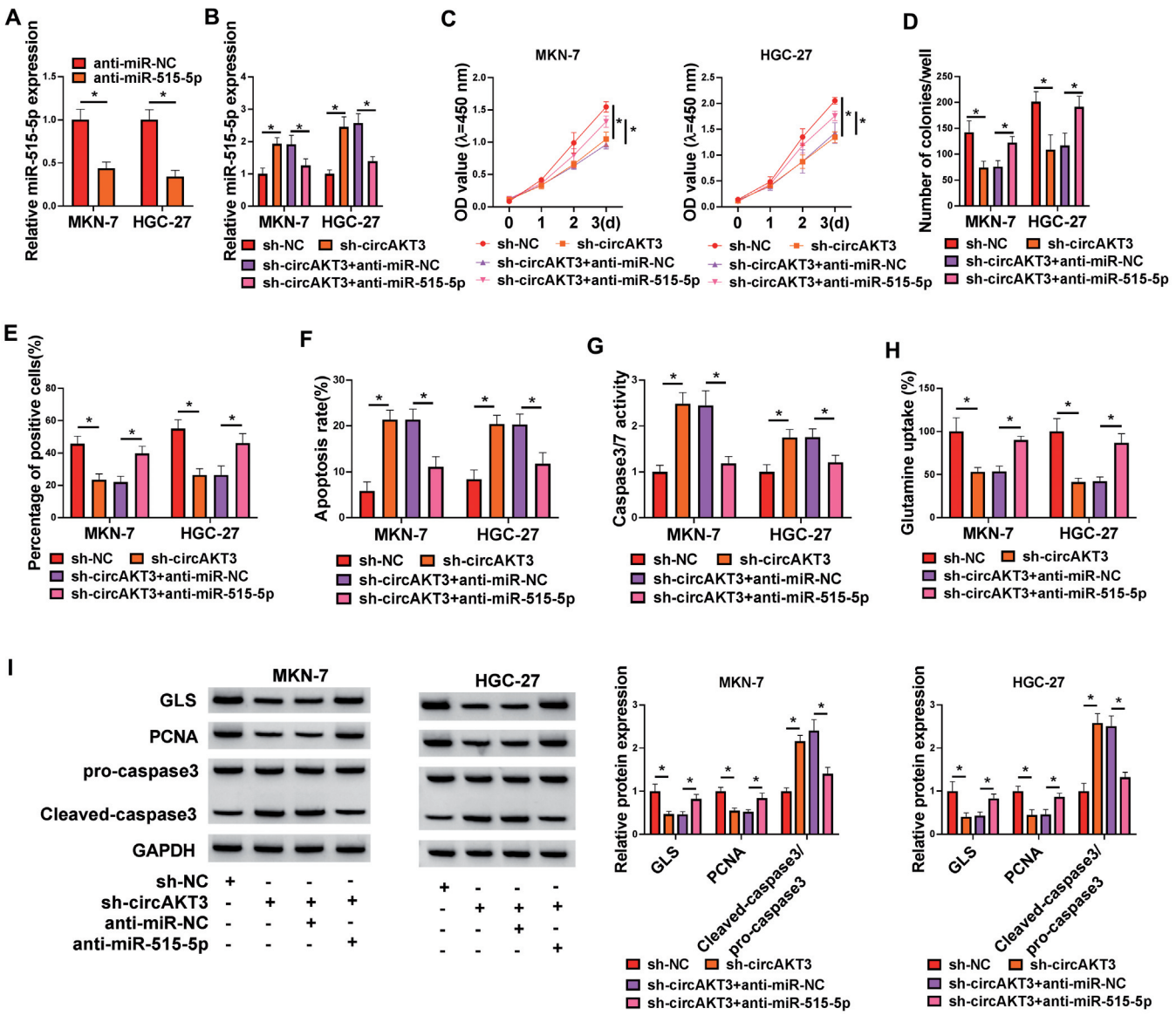

Fig. 6. MiR-515-5p depletion reversed the effects of circAKT3 knockdown on GC cell proliferation, survival and glutamine uptake. **A.** The expression of miR-515-5p in MKN-7 and HGC-27 cells transfected with anti-miR-515-5p or anti-miR-NC. **B.** The expression of miR-515-5p in MKN-7 and HGC-27 cells transfected with sh-circAKT3, sh-NC, sh-circAKT3+anti-miR-515-5p or sh-circAKT3+anti-miR-NC. In these transfected cells, cell proliferation was assessed by CCK-8 assay **(C)**, colony formation assay **(D)**, and EdU assay **(E)**. **F, G.** Cell apoptosis was determined by flow cytometry assay and caspase3/7 activity assay. **H.** Glutamine uptake was investigated using a commercial kit. **I.** The protein levels of GLS, PCNA and cleaved-caspase3 were detected by western blot. *P<0.05.

transfected cells. The data from CCK-8 assay, colony formation assay and EdU assay presented that cell proliferative capacity was suppressed by miR-515-5p restoration but impaired by SLC1A5 reintroduction (Fig. 9D,F; P<0.05). The data from flow cytometry assay and caspase3/7 activity assay revealed that miR-515-5p overexpression-induced MKN-7 and HGC-27 cell apoptosis was largely alleviated by the reintroduction of SLC1A5 (Fig. 9G,H and Fig. 10; P<0.05). In addition, glutamine uptake of MKN-7 and HGC-27 cells was effectively blocked by miR-515-5p restoration but restored by additional SLC1A5 overexpression (Fig. 9I; P<0.05). Furthermore, the protein levels of GLS and PCNA were reduced in MKN-7 and HGC-27 cells transfected with miR-515-5p but recovered in cells transfected with miR-515-5p+pcDNA-SLC1A5, while the protein level of cleaved-caspase3/pro-SLC1A5 was enhanced in MKN-7 and HGC-27 cells transfected with miR-515-5p but repressed in cells transfected with miR-515-5p+pcDNA-SLC1A5 (Fig. 9J; P<0.05). These data suggested that miR-515-5p overexpression inhibited GC cell proliferation, survival and glutamine metabolism by depleting SLC1A5.

CircAKT3 knockdown inhibited tumor growth in vivo

Animal models were established in nude mice to explore the role of circAKT3 in vivo. The data showed that circAKT3 downregulation in HGC-27 cells led to decreased tumor volume and tumor weight (Fig. 11A,B; P<0.05). The data from qPCR showed that the expression of circAKT3 was decreased, while the expression of miR-515-5p was enhanced in tumor tissues from the sh-circAKT3 group (Fig. 11C; P<0.05). The data from qPCR and western blot showed that the expression of SLC1A5 mRNA and protein was reduced in tumor tissues from the sh-circAKT3 group (Fig. 11C,D; P<0.05). Moreover, the data from IHC assay showed that the abundance of ki-67 and PCNA was strikingly decreased in tumor tissues from the sh-circAKT3 group relative to sh-NC group (Fig. 11E). The data manifested that circAKT3 knockdown inhibited tumor growth rate in vivo.

Discussion

The present study mainly discovered that circAKT3 was overexpressed in tumor tissues and cell lines of GC. Functional assays exhibited that circAKT3 downregulation inhibited GC cell proliferation, promoted cell apoptosis and blocked glutamine uptake. Mechanism analysis clarified that circAKT3 acted as an miR-515-5p sponge to increase the expression of SLC1A5, thus promoting the malignant behaviors of GC

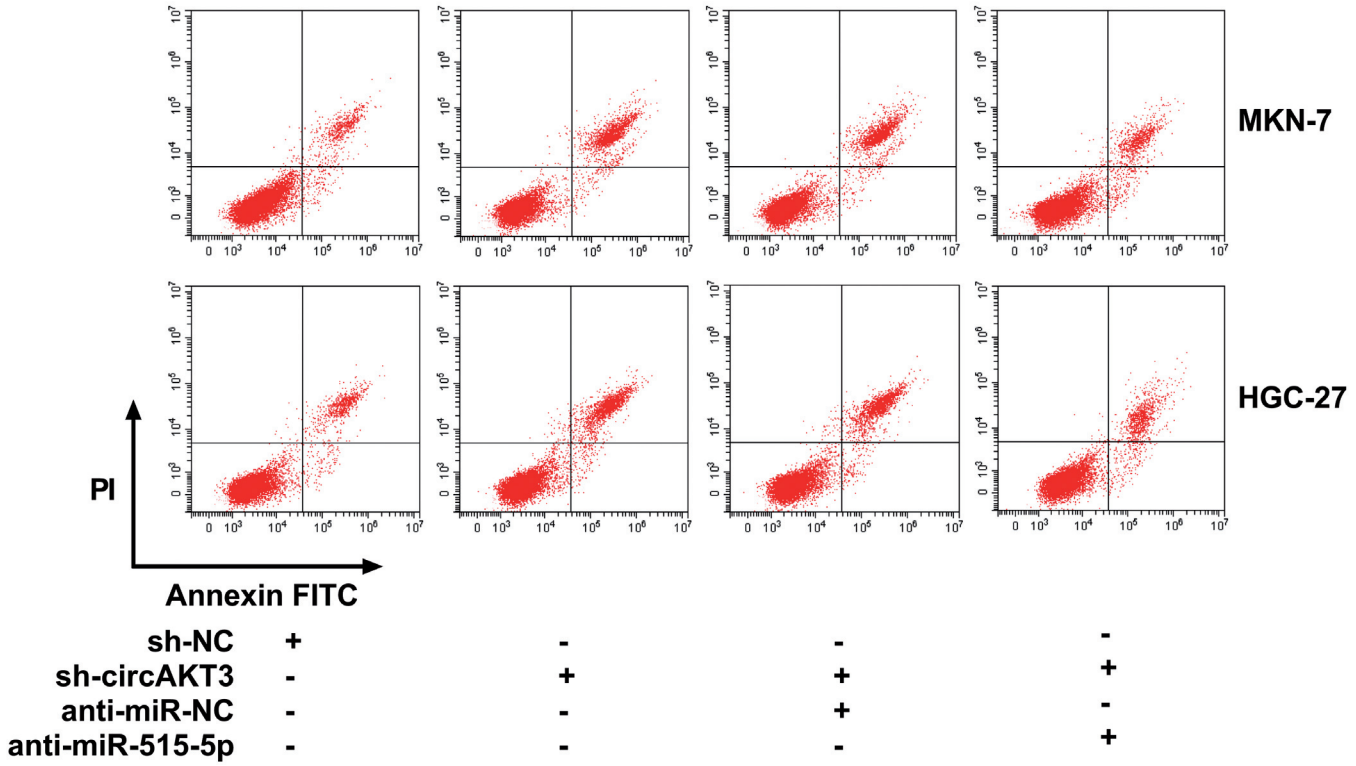

Fig. 7. Representative images of flow cytometry assay of MKN-7 and HGC-27 cells transfected with sh-circAKT3, sh-NC, sh-circAKT3+anti-miR-515-5p or sh-circAKT3+anti-miR-NC.

cells. Our study was the first to determine the role of circAKT3 on glutamine metabolism in GC cells and proposed a novel functional mechanism of circAKT3 in GC development.

CircAKT3 originates from the exon8 ~ exson11 regions of AKT3 gene by a back-splicing mechanism. CircAKT3 was previously identified to be notably upregulated in cisplatin-resistant tumor tissues of GC by circRNA sequencing analysis (Huang et al., 2019). Further analyses illustrated that circAKT3 upregulation promoted DNA damage repair and blocked the apoptosis of cisplatin-resistant GC cells, suggesting that circAKT3

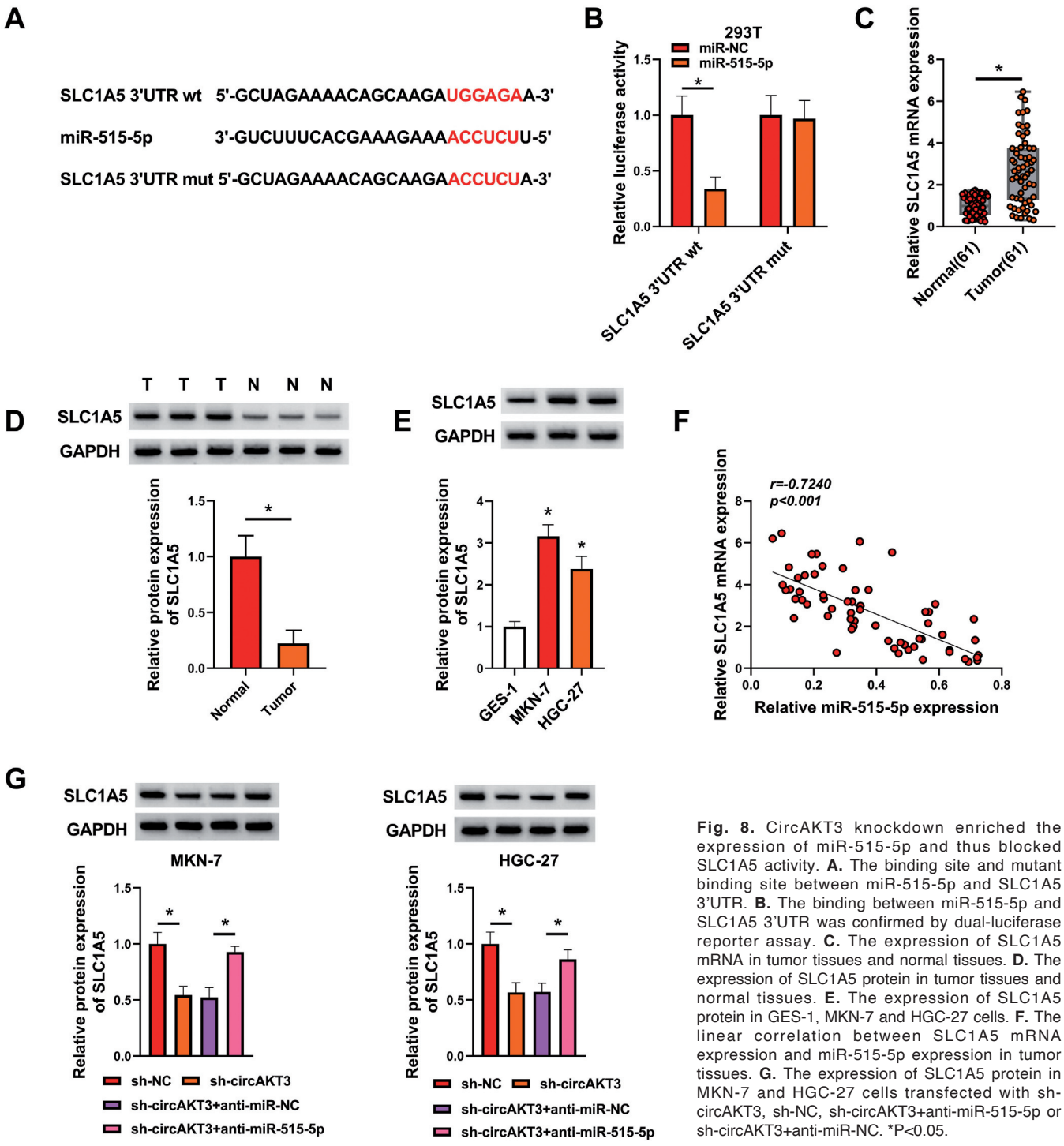

Fig. 8. CircAKT3 knockdown enriched the expression of miR-515-5p and thus blocked SLC1A5 activity. **A.** The binding site and mutant binding site between miR-515-5p and SLC1A5 3'UTR. **B.** The binding between miR-515-5p and SLC1A5 3'UTR was confirmed by dual-luciferase reporter assay. **C.** The expression of SLC1A5 mRNA in tumor tissues and normal tissues. **D.** The expression of SLC1A5 protein in tumor tissues and normal tissues. **E.** The expression of SLC1A5 protein in GES-1, MKN-7 and HGC-27 cells. **F.** The linear correlation between SLC1A5 mRNA expression and miR-515-5p expression in tumor tissues. **G.** The expression of SLC1A5 protein in MKN-7 and HGC-27 cells transfected with sh-circAKT3, sh-NC, sh-circAKT3+anti-miR-515-5p or sh-circAKT3+anti-miR-NC. *P<0.05.

dysregualtion was associated with the development of chemoresistance in GC (Huang et al., 2019). Interestingly, the role of circAKT3 was gradually clarified in other cancers. For instance, circAKT3 was overexpressed in exosomes of patients with oral squamous cell carcinoma (OSCC), and circAKT3 high expression was related to the adverse clinicopathologic features of OSCC patients (Luo et al., 2020). Similarly, circAKT3 was also upregulated in breast cancer samples, and circAKT3 knockdown repressed the proliferation, migration, invasion and chemoresistance of breast cancer cells (Li et al., 2021). Consistent with these findings, our study determined that circAKT3 was highly expressed in GC tumor tissues and cell lines, and its deficiency suppressed GC cell proliferation and survival. Besides, we found that circAKT3 knockdown impaired glutamine uptake of GC cells, suggesting that circAKT3 regulated glutamine energy metabolism to modulate cell growth. In addition, the tumorigenicity of circAKT3 in GC was also verified by animal models. These data highlighted that circAKT3 expression was aberrantly increased in tumor tissues, and its downregulation largely attenuated tumor malignant behaviors, suggesting that circAKT3 was a wide oncogenic driver, which needed to be further verified in other cancers.

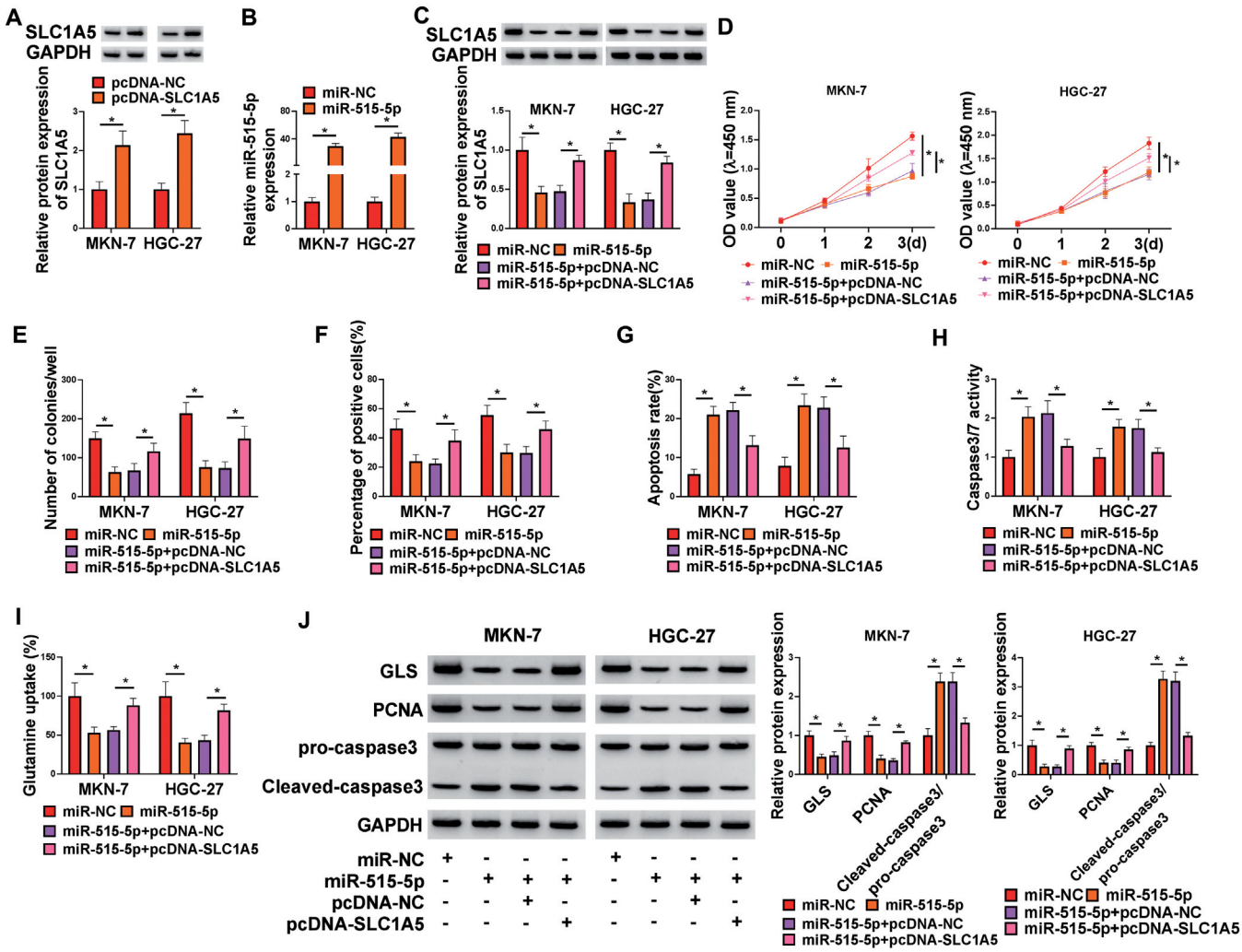

Fig. 9. SLC1A5 overexpression reversed the effects of miR-515-5p restoration on GC cell proliferation, survival and glutamine uptake. **A.** The expression of SLC1A5 protein in MKN-7 and HGC-27 cells transfected with pcDNA-SLC1A5 or pcDNA-NC. **B.** The expression of miR-515-5p in MKN-7 and HGC-27 cells transfected with miR-515-5p or miR-NC. **C.** The expression of SLC1A5 protein in MKN-7 and HGC-27 cells transfected with miR-515-5p, miR-NC, miR-515-5p+pcDNA-SLC1A5 or miR-515-5p+pcDNA-NC. **D-F.** Cell proliferation in these transfected cells was assessed by CCK-8 assay, colony formation assay and EdU assay. **G, H.** Cell apoptosis in these transfected cells was assessed by flow cytometry assay and caspase3/7 activity. **I.** Glutamine uptake was determined using a commercial kit. **J.** The protein levels of GLS, PCNA and cleaved-caspase3 were detected by western blot. *P<0.05.

It has been published that circAKT3 confers cisplatin resistance in GC by targeting the miR-198/PIK3R1 pathway (Huang et al., 2019). To further excavate the regulatory networks of circAKT3, we screened the target miRNAs of circAKT3. Bioinformatics tool determined that miR-515-5p was one of the targets of circAKT3, which was validated by dual-luciferase reporter assay and RIP assay. Given that miR-515-5p depletion was reported to promote the proliferation of GC cells (Zhang et al., 2019a,b), we believed that miR-515-5p was involved in GC development. Rescue experiments discovered that the inhibitory proliferation, survival and glutamine metabolism of GC cells caused by circAKT3 knockdown were substantially recovered by miR-515-5p inhibition, while miR-515-5p overexpression largely suppressed these malignant cell behaviors, indicating that miR-515-5p was a tumor suppressor in GC. CircAKT3 facilitated the growth of GC via the target inhibition on miR-515-5p. The tumor suppressor role of miR-515-5p has been clarified in various cancers, such as prostate cancer, lung cancer and breast cancer (Pinho et al., 2013; Pardo et al., 2016; Zhang et al., 2019a,b). The data suggested that miR-515-5p-based target therapy might be a novel strategy in cancer treatment.

SLC1A5 (ASCT2) has been mentioned to be essential for glutamine transport and amino acid metabolism in diverse cancer cells (Lin et al., 2018). The knockdown of SLC1A5 inhibited cell growth and glutamine transport but induced cell apoptosis and cell cycle arrest in esophageal cancer (Lin et al., 2018). Besides, the target inhibition of SLC1A5 blocked glutamine metabolism-dependent lung cancer cell growth and survival (Hassanein et al., 2013). In GC, high levels of SLC1A5 were shown in human GC tissues, and the depletion of SLC1A5 effectively inhibited glutamine uptake and GC cell growth (Ye et al., 2018; Wang et al., 2019a,b). These consequences demonstrated that SLC1A5 promoted cancer cell growth mainly by activating glutamine metabolism. In our study, we found that miR-515-5p inhibited the expression of SLC1A5 by binding to its 3'UTR. However, circAKT3 was able to act as miR-515-5p sponge and thus relieved the inhibition of miR-515-5p on SLC1A5.

Though our study provides enough evidence to understand the role and regulatory mechanism of circAKT3 in GC, there are still some limitations. For instance, the correlation between circAKT3 expression and clinicopathological feathers of GC cases is lacking. Besides, some typical cancer-related signaling pathways are not explored. These limitations should be addressed

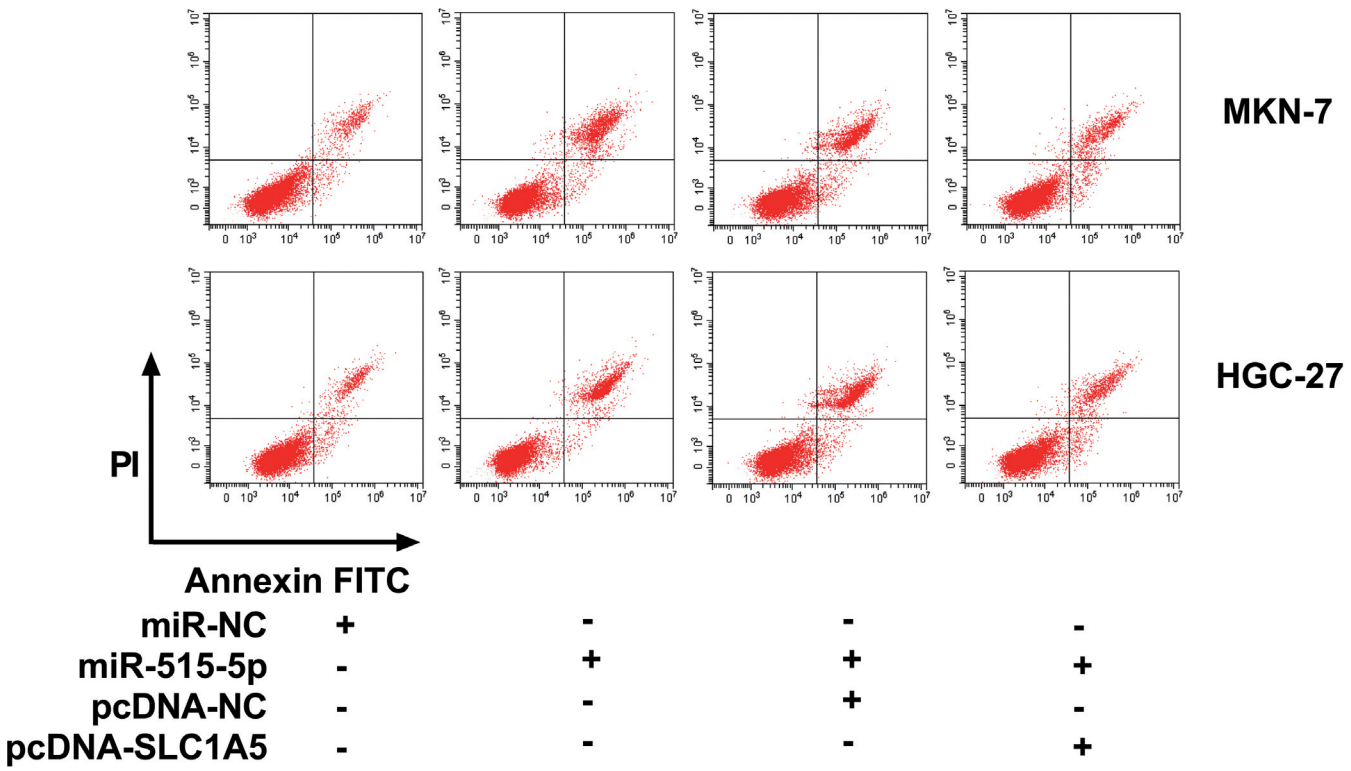

Fig. 10. Representative images of flow cytometry assay of MKN-7 and HGC-27 cells transfected with miR-515-5p, miR-NC, miR-515-5p+pcDNA-SLC1A5 or miR-515-5p+pcDNA-NC.

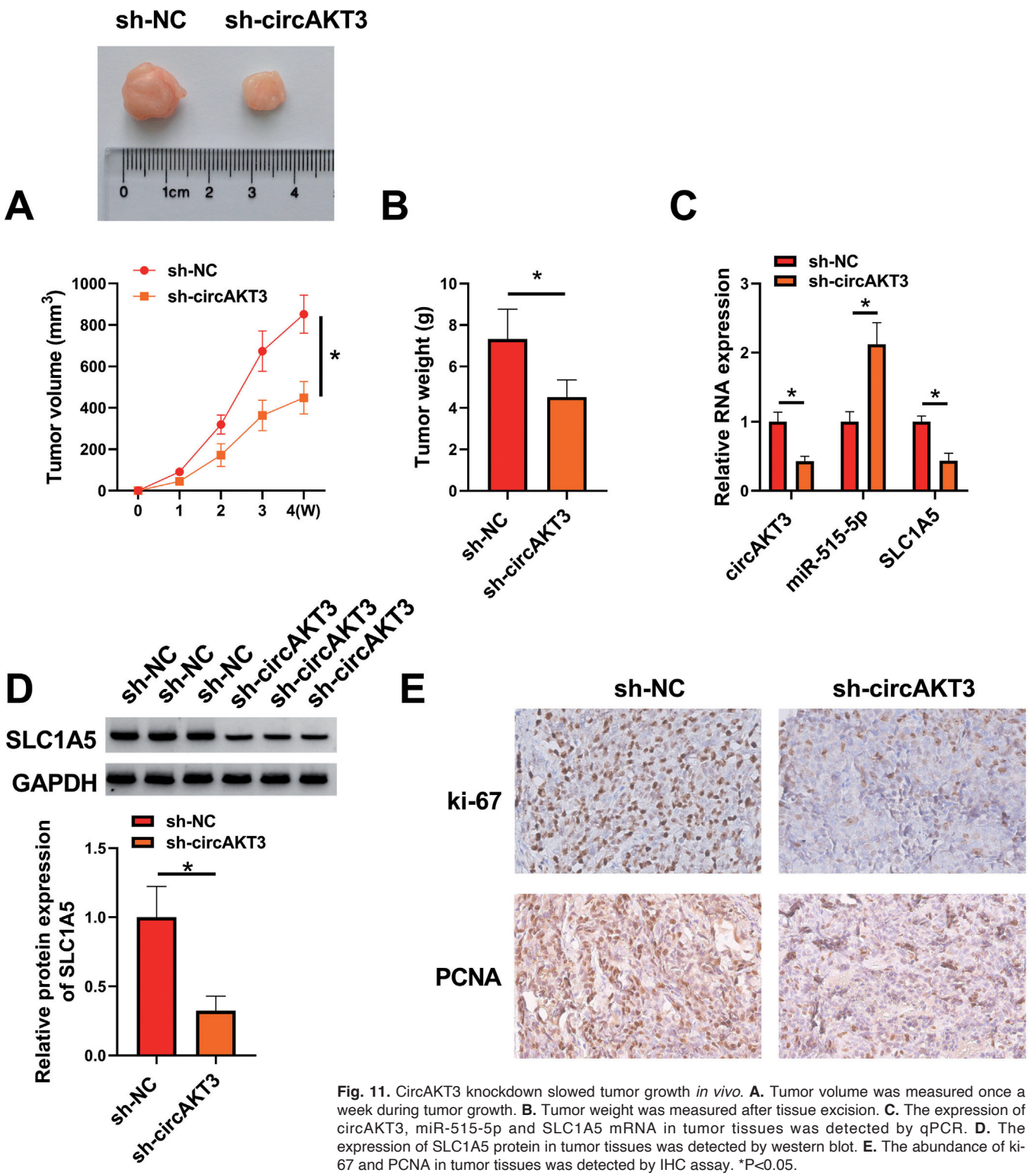

Fig. 11. CircAKT3 knockdown slowed tumor growth *in vivo*. **A.** Tumor volume was measured once a week during tumor growth. **B.** Tumor weight was measured after tissue excision. **C.** The expression of circAKT3, miR-515-5p and SLC1A5 mRNA in tumor tissues was detected by qPCR. **D.** The expression of SLC1A5 protein in tumor tissues was detected by western blot. **E.** The abundance of ki-67 and PCNA in tumor tissues was detected by IHC assay. *P<0.05.

in further work.

Conclusion

Collectively, circAKT3 was overexpressed in tumor tissues and cell lines of GC. CircAKT3 knockdown inhibited GC cell proliferation, survival and glutamine metabolism. CircAKT3 might serve as an oncogenic driver to accelerate the malignant development of GC by increasing the expression of SLC1A5 via targeting miR-515-5p. Our study further understood the role of circAKT3 in GC, and circAKT3 inhibition might be a strategy for the treatment of GC.

Data Availability Statement. The datasets used and analyzed during the current study are available from the corresponding author on reasonable request.

Conflicts of interest. The authors have no conflict of interest to declare.

References

Dudekula D.B., Panda A.C., Grammatikakis I., De S., Abdelmohsen K. and Gorospe M. (2016). CircInteractome: A web tool for exploring circular RNAs and their interacting proteins and microRNAs. RNA Biol. 13, 34-42.

Feng W., Ding Y., Zong W. and Ju S. (2019). Non-coding RNAs in regulating gastric cancer metastasis. Clin. Chim. Acta 496, 125-133.

Hassanein M., Hoeksema M.D., Shiota M., Qian J., Harris B.K., Chen H., Clark J.E., Alborn W.E. Eisenberg R. and Massion P.P. (2013). SLC1A5 mediates glutamine transport required for lung cancer cell growth and survival. Clin. Cancer Res. 19, 560-570.

Huang X., Li Z., Zhang Q., Wang W., Li B., Wang L., Xu Z., Zeng A., Zhang X., Zhang X., He Z., Li Q., Sun G., Wang S., Li Q., Wang L., Zhang L., Xu H. and Xu Z. (2019). Circular RNA AKT3 upregulates PIK3R1 to enhance cisplatin resistance in gastric cancer via miR-198 suppression. Mol. Cancer. 18, 71.

Jie M., Wu Y., Gao M., Li X., Liu C., Ouyang Q., Tang Q., Shan C., Lv Y., Zhang K., Dai Q., Chen Y., Zeng S., Li C., Wang L., He F., Hu C. and Yang S. (2020). CircMRPS35 suppresses gastric cancer progression via recruiting KAT7 to govern histone modification. Mol. Cancer. 19, 56.

Khanipouyani F., Akrami H. and Fattahi M.R. (2021). Circular RNAs as important players in human gastric cancer. Clin. Transl. Oncol. 23, 10-21.

Li J.H., Liu S., Zhou H., Qu L.H. and Yang J.H. (2014). starBase v2.0: decoding miRNA-ceRNA, miRNA-ncRNA and protein-RNA interaction networks from large-scale CLIP-Seq data. Nucleic Acids Res. 42, (Database issue), D92-97.

Li H., Xu W., Xia Z., Liu W., Pan G., Ding J., Li J., Wang J., Xie X. and Jiang D. (2021). Hsa_circ_0000199 facilitates chemo-tolerance of triple-negative breast cancer by interfering with miR-206/613-led PI3K/Akt/mTOR signaling. Aging (Albany NY). 13, 4522-4551.

Lin J., Yang T., Peng Z., Xiao H., Jiang N., Zhang L., Ca D., Wu P. and Pan Q. (2018). SLC1A5 silencing inhibits esophageal cancer growth via cell cycle arrest and apoptosis. Cell Physiol. Biochem. 48, 397.

Liu J., Liu T., Wang X. and He A. (2017). Circles reshaping the RNA world: from waste to treasure. Mol. Cancer. 16, 58.

Luo Y., Liu F., Guo J. and Gui R. (2020). Upregulation of circ_0000199 in circulating exosomes is associated with survival outcome in OSCC. Sci. Rep. 10, 13739.

Pardo O.E., Castellano L., Munro C.E., Hu Y., Mauri F., Krell J., Lara R., Pinho F.G., Choudhury T., Frampton A.E., Pellegrino L., Pshezhetskiy D., Wang Y., Waxman J., Seckl M.J. and Stebbing J. (2016). miR-515-5p controls cancer cell migration through MARK4 regulation. EMBO Rep. 17, 570-584.

Pinho F.G., Frampton A.E., Nunes J., Krell J., Alshaker H., Jacob J., Pellegrino L., Roca-Alonso L., de Giorgio A., Harding V., Waxman J., Stebbing J., Pchejetski D. and Castellano L. (2013). Downregulation of microRNA-515-5p by the estrogen receptor modulates sphingosine kinase 1 and breast cancer cell proliferation. Cancer Res. 73, 5936-5948.

Ruan Y., Li Z., Shen Y., Li T., Zhang H. and Guo J. (2020). Functions of circular RNAs and their potential applications in gastric cancer. Expert Rev. Gastroenterol. Hepatol. 14, 85-92.

Smyth E.C., Nilsson M., Grabsch H.I., van Grieken N.C. and Lordick F. (2020). Gastric cancer. Lancet. 396, 635-648.

Sung H., Ferlay J., Siegel R.L., Laversanne M., Soerjomataram I., Jemal A. and Bray F. (2021). Global cancer statistics 2020: GLOBOCAN estimates of incidence and mortality worldwide for 36 cancers in 185 countries. CA Cancer J. Clin. 71, 209-249.

Tang X., Zhu J., Liu Y., Chen C., Liu T. and Liu J. (2019). Current understanding of circular RNAs in gastric cancer. Cancer Manag. Res. 11, 10509-10521.

Wang S., Tang D., Wang W., Yang Y., Wu X., Wang L. and Wang D. (2019a). circLMTK2 acts as a sponge of miR-150-5p and promotes proliferation and metastasis in gastric cancer. Mol. Cancer 18, 162.

Wang L., Liu Y., Zhao T.L., Li Z.Z., He J.Y., Zhang B.J., Du H.-Z., Jiang J.-W., Yuan S.-T. and Sun L. (2019b). Topotecan induces apoptosis via ASCT2 mediated oxidative stress in gastric cancer. Phytomedicine 57, 117-128.

Wang D., Liu K., and Chen E. (2020). LINC00511 promotes proliferation and invasion by sponging miR-515-5p in gastric cancer. Cell Mol. Biol. Lett. 25, 4.

Wei L., Sun J., Zhang N., Zheng Y., Wang X., Lv L., Liu J., Xu Y., Shen Y. and Yang M. (2020). Noncoding RNAs in gastric cancer: implications for drug resistance. Mol. Cancer. 19, 62.

Ye J., Huang Q., Xu J., Huang J., Wang J., Zhong W., Chen W., Lin X. and Lin X. (2018). Targeting of glutamine transporter ASCT2 and glutamine synthetase suppresses gastric cancer cell growth. J. Cancer Res. Clin. Oncol. 144, 821-833.

Zhang H., Wang X., Huang H., Wang Y., Zhang F. and Wang S. (2019a). Hsa_circ_0067997 promotes the progression of gastric cancer by inhibition of miR-515-5p and activation of X chromosome-linked inhibitor of apoptosis (XIAP). Artif. Cells Nanomed. Biotechnol. 47, 308-318.

Zhang X., Zhou J., Xue D., Li Z., Liu Y. and Dong L. (2019b). MiR-515-5p acts as a tumor suppressor via targeting TRIP13 in prostate cancer. Int. J. Biol. Macromol. 129, 227-232.

Accepted December 1, 2021